

### Supporting Information for World Wide Web Edition

Nondenaturing second-round gels performed with inclusion of various concentrations of monovalent cations ( $\text{Na}^+$  or  $\text{K}^+$ ) in the running buffer are shown in Figure 1. Inclusion of monovalents did not change the rank order of mobilities for the various P4-P6 derivatives.

Tables of  $\Delta\Delta G^{\circ}$  values with error estimates for all P4-P6 samples are in Table 1. Because  $[\text{Mg}^{2+}]_{1/2}$  values were determined from the fit values of  $K$  and  $n$  (manuscript Figure 4), and because  $\Delta G^{\circ}$  is related to the logarithm of  $[\text{Mg}^{2+}]_{1/2}$  by eq (3) of the manuscript, the error on all  $\Delta G^{\circ}$  values is in general asymmetrical. However, in all cases for which  $\Delta\Delta G^{\circ}$  is  $< 2.4$  kcal/mol (that is, all the data shown in manuscript Figure 5), the plus and minus errors were approximately equal and almost always  $\leq 0.2$  kcal/mol.

Hill coefficients for the titration data (manuscript Figure 4) were determined in two ways. The first method was to fit the titration data directly (four-parameter fit, as described in Materials and Methods). The second method used the fit values of  $M_{\text{low}}$  and  $M_{\text{high}}$  to calculate  $\log((M_{\text{obs}} - M_{\text{low}})/(M_{\text{high}} - M_{\text{obs}}))$ . A Hill plot was then obtained by plotting this value versus  $\log[\text{Mg}^{2+}]$ ; the slope of the plot (central data points only) is the Hill coefficient  $n$ . Representative Hill plots determined by this latter method are shown in Figure 2. The values of  $n$  calculated by both methods for the various P4-P6 samples of Table 1 are shown in Figure 3; little difference is observed. The Hill coefficients determined by the two methods show a reasonable correlation (Figure 4).

Table 1: Destabilization of P4-P6 RNA Tertiary Folding at 35 °C by 2'-Deoxy and 2'-Methoxy Substitutions <sup>a</sup>									
site(s) substituted	$\Delta\Delta G^{o,b}$	error estimates <sup>b</sup>	site(s) substituted	$\Delta\Delta G^{o,b}$	error estimates <sup>b</sup>				
<b>Round 1</b>									
1	C109-2'-OMe	1.06	+0.05	-0.05	8	A183:A184-2'-OMe	1.27	+0.15	-0.11
2	G110-2'-OMe	0.81	+0.08	-0.08	9	C109:A183-2'-OMe	0.68	+0.14	-0.16
3	C109;G110-2'-OMe	1.14	+0.08	-0.07	10	C109:A184-2'-OMe	0.77	+0.12	-0.13
4	C137-2'-OMe	2.42	+0.56	-0.35	11	C109:A183: A184-2'-OMe	0.27	+0.19	-0.22
5	A183-2'-OMe	0.81	+0.06	-0.06	12	G110:A183-2'-OMe	0.02	+0.23	-0.26
6	A184-2'-OMe	0.78	+0.07	-0.08	13	G110:A184-2'-OMe	1.17	+0.14	-0.10
7	A186-2'-OMe	4.13	+1.01	-0.58	14	G110:A183: A184-2'-OMe	0.79	+0.10	-0.10
					15	C109;G110:	0.32	+0.18	-0.21
					16	A183-2'-OMe C109;G110:	0.80	+0.10	-0.11
					17	A184-2'-OMe C109;G110:	-0.11	+0.25	-0.28
					18	A183:A184-2'-OMe C137-2'-OMe	2.74	+0.76	-0.45
					19	A186-2'-OMe	4.14	+1.13	-0.53
<b>Round 3</b>									
20	C109-2'-H	0.40	+0.13	-0.13	35	A183-2'-H	0.17	+0.16	-0.16
21	G110-2'-H	0.91	+0.13	-0.12	36	C109:A183-2'-H	0.73	+0.14	-0.14
22	C109;G110-2'-H	1.32	+0.15	-0.16	37	C109:A184-2'-H	1.18	+0.14	-0.13
23	A184-2'-H	1.12	+0.13	-0.14	38	G110:A183-2'-H	1.27	+0.15	-0.14
24	G110:A184-2'-H	1.42	+0.16	-0.18	39	A183:A184-2'-H	1.98	+0.18	-0.17
25	A183:A184-2'-OMe	1.06	+0.13	-0.13	40	C109;G110: A183-2'-H	1.69	+0.19	-0.17
<b>Round 4</b>									

26	G110:A183-2'-OMe	0.12	+0.19	-0.19	41	C109:G110: A184-2'-H	1.84	+0.22	-0.19
27	C109:G110: A183:A184-2'-OMe	-0.20	+0.20	-0.22	42	C109:A183: A184-2'-H	1.75	+0.22	-0.19
28	U107-2'-OMe	0.07	+0.17	-0.18	43	G110:A183: A184-2'-H	2.24	+0.26	-0.22
29	A114-2'-OMe	0.04	+0.19	-0.20	44	C109:G110: A183:A184-2'-H	2.27	+0.25	-0.21
30	G188-2'-OMe	0.29	+0.15	-0.16	45	G110-2'-OMe	0.75	+0.13	-0.13
31	C193-2'-OMe	0.10	+0.17	-0.18	46	C109-2'-H	0.40	+0.12	-0.13
32	C109-2'-OMe	1.03	+0.13	-0.14	47	C109:G110-2'-OMe	1.22	+0.16	-0.15
33	C137-2'-OMe	2.36	+0.34	-0.49	48	G110-2'-H	1.03	+0.14	-0.13
34	A186-2'-OMe	3.99	+0.65	-1.04	49	C109:G110: A183-2'-OMe	0.28	+0.15	-0.16
					50	C109:G110-2'-H	1.55	+0.21	-0.18
					51	G110:A184-2'-H	1.72	+0.28	-0.22

<sup>a</sup> Derivatives are listed in the order shown on the gels of manuscript Figure 3, followed by other samples not shown in those gels. Derivatives are identified by a number for cross-referencing to Supporting Information Figure 3. <sup>b</sup> kcal/mol. We report  $\Delta\Delta G^\circ$  values to one significant figure more than is arguably appropriate so that rounding errors do not affect comparison of the values.

4

### Supporting Information Figure Legends

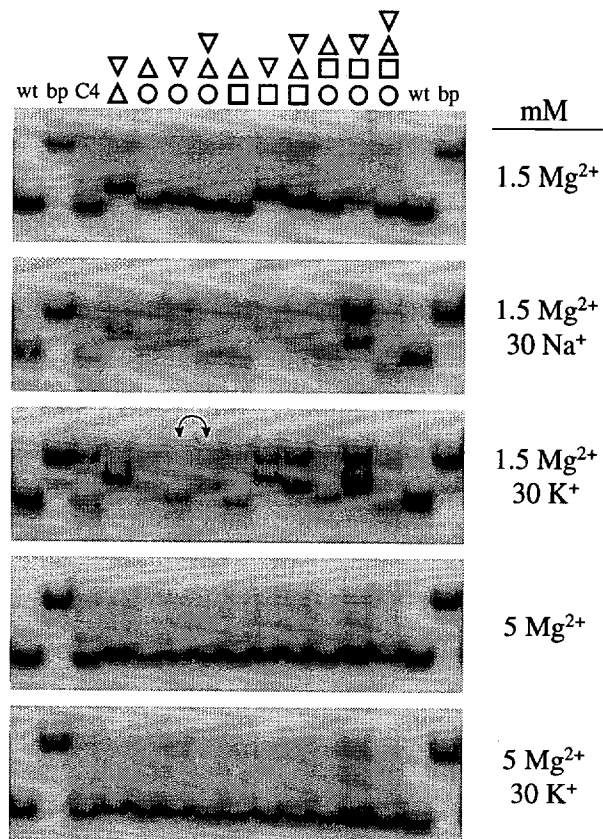
Figure 1: Nondenaturing gels of P4-P6 derivatives with varying concentrations of monovalent ions. Second-round gels with  $Mg^{2+}$  plus varying concentrations of  $Na^+$  or  $K^+$  are shown; see manuscript Figure 3 for symbols. The double-headed arrow on the third gel indicates two samples accidentally switched during the gel loading.

Figure 2: Representative Hill plots for the native gel titration data. Six plots from the Round 3 data are shown.

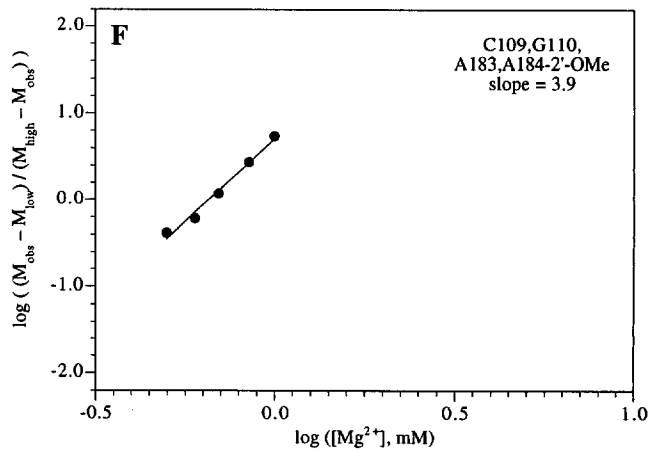
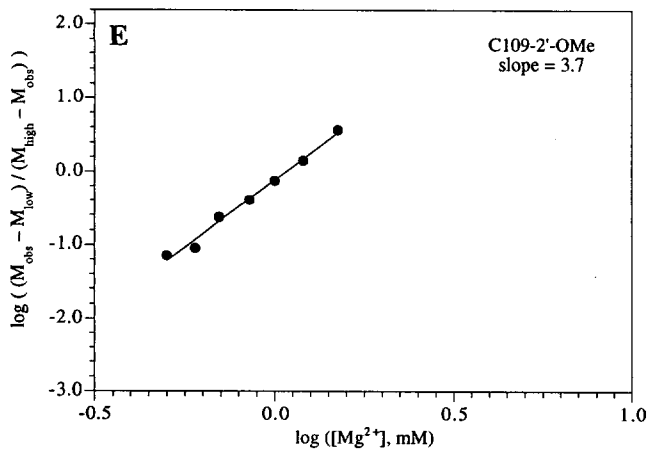
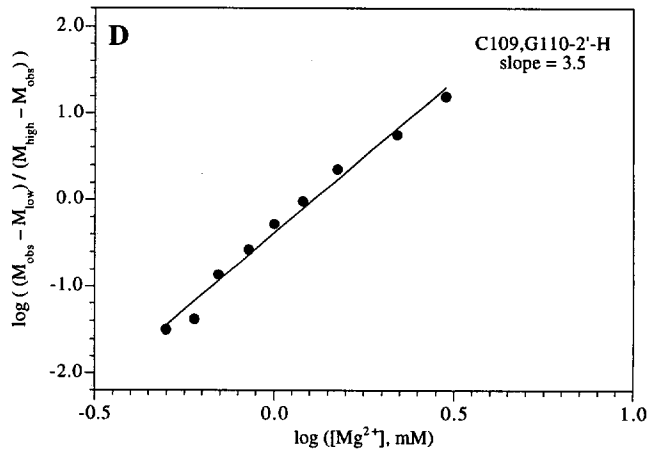
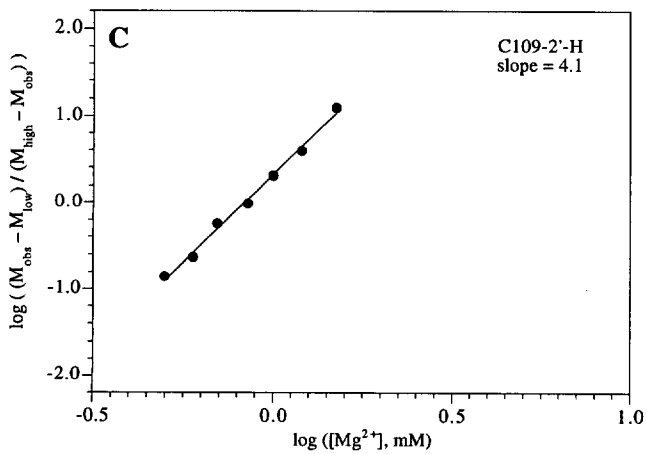
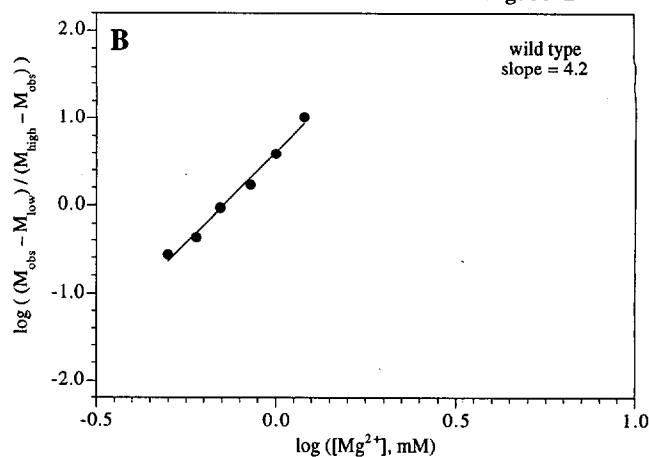
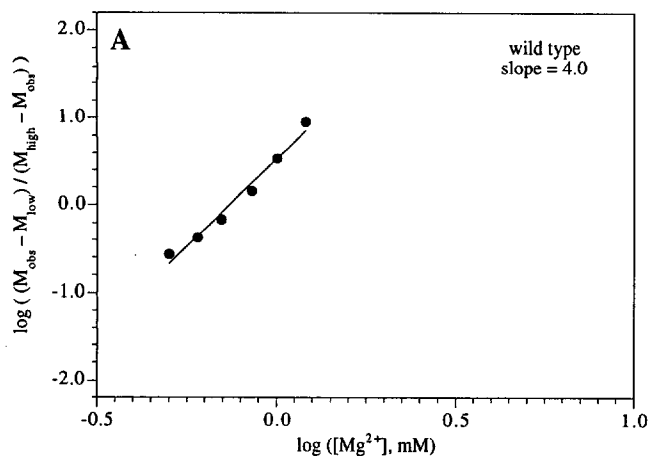
Figure 3: Comparison of Hill coefficients determined from titration data and from Hill plots. (A) Round 1 gels. (B) Round 2 gels. (C) Round 3 gels. (D) Round 4 gels. Error bars are  $\pm \sigma$ . Samples are labelled with "w" followed by a number for authentic wild-type P4-P6 samples; "c" followed by a number for the control wild-type P4-P6 RNAs C1-C5 prepared by ligation; and with numbers 1-51 for the P4-P6 derivatives as listed in Table 1.

Figure 4: Correlation of Hill coefficients determined from titration data and from Hill plots. Data taken from Figure 2. Different symbols are used for Rounds 1-4 data as shown. The best fit line is  $n_{Hill} = -0.213 + 1.054 \cdot n_{tit}$ , with correlation coefficient  $R = 0.78$ .

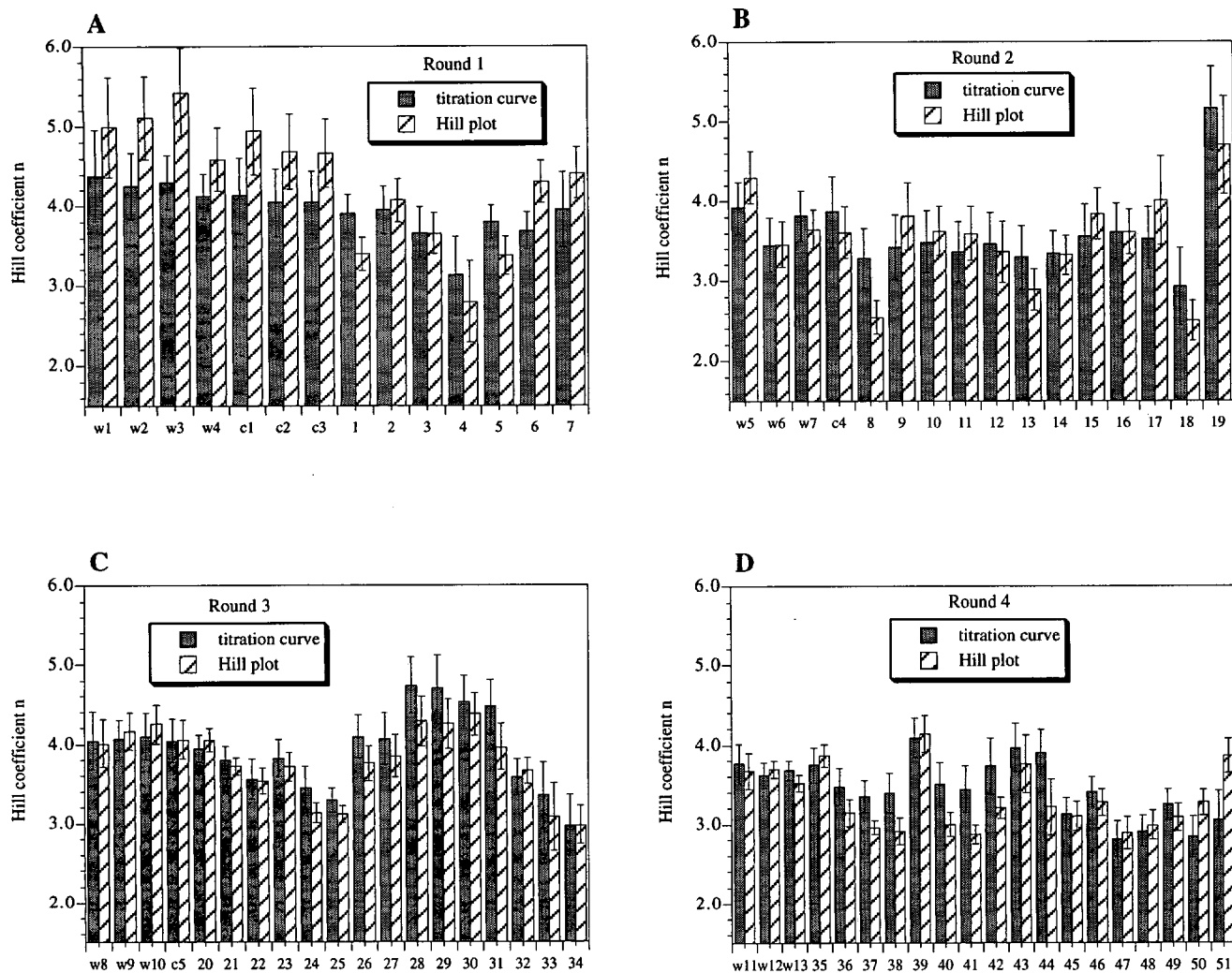
Silverman & Cech  
Supp Info  
Figure 1



Silverman & Cech  
Supp Info  
Figure 2



Silverman & Cech  
Supp Info  
Figure 3



Silverman & Cech  
Supp Info  
Figure 4

